

# pseudo-Bayesian Neural Networks for detecting Out of Distribution Inputs

Gagandeep Singh

singh.23@iitj.ac.in

Indian Institute of Technology, Jodhpur  
Rajasthan, India

Deepak Mishra

dmishra@iitj.ac.in

Indian Institute of Technology, Jodhpur  
Rajasthan, India

## Abstract

Conventional Bayesian Neural Networks (BNNs) are known to be capable of providing multiple outputs for a single input, the variations in which can be utilised to detect Out of Distribution (OOD) inputs. BNNs are difficult to train due to their sensitivity towards the choice of priors. To alleviate this issue, we propose *pseudo*-BNNs where instead of learning distributions over weights, we use point estimates and perturb weights at the time of inference. We modify the cost function of conventional BNNs and use it to learn parameters for the purpose of injecting right amount of random perturbations to each of the weights of a neural network with point estimate. In order to effectively segregate OOD inputs from In Distribution (ID) inputs using multiple outputs, we further propose two measures, derived from the index of dispersion and entropy of probability distributions, and combine them with the proposed *pseudo*-BNNs. Overall, this combination results in a principled technique to detect OOD samples at the time of inference. We evaluate our technique on a wide variety of neural network architectures and image classification datasets. We observe that our method achieves state of the art results and beats the related previous work on various metrics such as FPR at 95% TPR, AUROC, AUPR and Detection Error by just using 2 to 5 samples of weights per input.

## 1. Introduction

Neural networks have been shown to perform well when the testing data is sampled from a distribution which is same or approximately similar to the training data distribution [16, 25, 9, 5, 30]. However, the performance drops by a large margin when the testing data comes from a distribution which is far away from that of the training data [22, 10], also called as Out of Distribution (OOD) data. Therefore, in real world systems there is no guarantee on how a network will behave because, it is often difficult to ensure the similarity of training and test data distributions [1]. Thus, it is

important to make neural networks less prone to failure i.e., confidently making wrong predictions for OOD inputs.

Conventional BNNs facilitate the detection of OOD inputs as they allow sampling of weights at the time of inference from the distributions (Gaussian) learned during training and provide multiple outputs for individual inputs. Large variations in the outputs of a single input reflects OOD instance. However, BNNs are sensitive to the choice of prior distribution over their weights, leading to difficulties in training. Hence, to reduce the training effort, we propose to re-use already trained frequentist neural networks or simply Artificial Neural Networks (ANNs) with point estimate and learn parameters to inject random perturbations (Gaussian) to their weights for obtaining multiple weight samples during inference. For this purpose, we use a modified version of the traditional cost function of BNNs. We call the networks so obtained as *pseudo*-BNNs because, their training methods are different from conventional BNNs but their inference algorithms are the same i.e., for each input multiple samples of weights are drawn and the average of all the different outputs obtained from each of those samples is used as the final output. Specifically, a *pseudo*-BNN has two parameters  $(\mu, \sigma)$  and each of its weight is sampled as  $\mu + \sigma \circ \epsilon$ ,  $\epsilon \sim N(0, 1)$  which is the same as reparametrization trick [13] where  $\mu$  is taken from a point estimation of ANN and  $\sigma$  is optimised over our proposed cost function. It is note worthy that since  $\mu$  is already optimised over the training data, hence by clever use of initializers, the training effort for  $\sigma$  can be reduced significantly.

Since, multiple weight samples lead to different final outputs, a posterior distribution in case of classifier neural networks, we quantify the variations in these outputs to flag OOD inputs. In order to do so, we propose two measures of disagreements derived from index of dispersion and entropy of probability distributions.

We evaluate our technique on four classifier neural network architectures, simple convolution neural networks (CNN) [4], VGG-10 [25], ResNet-20 [9] and DenseNet-100

[11]. We use MNIST [17], CIFAR10 [14], SVHN [21], CIFAR100 [15] as ID datasets and Fashion-MNIST [28], CIFAR100 [28], CMATERDB [7], Gaussian images, where each pixel is sampled from  $N(0, 1)$ , as OOD datasets. We observed that our technique considerably improvises on previous works related to OOD input detection. For example, the False Positive Rate at 95% True Positive Rate, for MNIST as ID and Fashion-MNIST as OOD data, was found to be 1.72% by using just 2 to 5 samples of weights as compared to 27.48% from the baseline method [10]. We have presented a principled analysis of our approach by taking ideas from Bernstein *et al.* [2].

In summary our main contributions are as follows,

- We have modified the cost function used in the training of Gaussian BNNs, in order to learn a second parameter for the purpose of injecting random perturbations to the weights of an ANN with point estimate at the time of inference for obtaining multiple outputs for an input without compromising on test accuracy. We call the resulting network as *pseudo*-BNN.
- We propose measures of disagreement to quantify the variations in the outputs of a *pseudo*-BNN to effectively flag OOD inputs.
- We have presented a principled analysis of our technique in order to explain the results obtained.

The rest of the paper is organised as follows. In Section 2 we have formalised the problem of OOD input detection and explained the mathematical aspects of our technique. In Section 3, we have briefly explained the related previous work and wherever possible we have also presented a comparison with ours. In Section 4, we have described about the details of our experiments and showcased our results and comparisons with the state of the art methods. In Section 5, we have discussed the principles behind our technique and hence, explained the results obtained. In the last section, we conclude the paper by presenting some advantages in disguise of our work.

## 2. Problem Formulation and Proposed Solution

Let  $C$  be a classifier neural network,  $T_r$  and  $T_e$  be the training and test data distributions respectively,  $X$  be a sample from one of  $T_r$  and  $T_e$ ,  $M$  be a real valued measure and  $\delta$  be a real number, then the problem of OOD input detection can be defined as follows,

**OOD Input Detection** - If  $C$  is trained on data which is sampled from  $T_r$  and receives  $X$  sampled from  $T_e$  then  $M < \delta$  should hold.

We have attempted to solve the special case of the above problem, where  $C$  applies softmax activation on its outputs

and  $T_r$  and  $T_e$  are defined on image space. As a first step, we developed *pseudo*-BNN which are described in detail below.

### 2.1. *pseudo*-BNN

In principle, conventional BNNs optimize their parameters over the following cost function which is also known as variational free energy [20, 29, 8] or the expected lower bound [24, 29, 12],

$$F(D, \theta) = KL[q(\mathbf{w}|\theta) || P(\mathbf{w})] - E_{q(\mathbf{w}|\theta)}[\log P(D|\mathbf{w})] \quad (1)$$

In (1),  $D$  denotes the training data,  $q(\mathbf{w}|\theta)$  and  $P(\mathbf{w})$  are the posterior distribution and prior over the weights respectively, where  $\theta$  is the tuple of parameters of the posterior distribution,  $-E_{q(\mathbf{w}|\theta)}[\log P(D|\mathbf{w})]$  is the negative log likelihood over the data given the weights. It is basically the sum of two parts, the data dependent part which is called as likelihood cost and the prior dependent part which is called as complexity cost [3].

In practice, the cost function in (1) is intractable and hence, the following approximated cost function is used [3],

$$F(D, \theta) \approx \sum_{i=1}^n \log q(\mathbf{w}^{(i)}|\theta) - \log P(\mathbf{w}^{(i)}) - \log P(D|\mathbf{w}^{(i)}) \quad (2)$$

In (2),  $\mathbf{w}^{(i)}$  is the  $i^{th}$  Monte Carlo sample of weights drawn from the posterior  $q(\mathbf{w}^{(i)}|\theta)$ . We consider the case when  $q(\mathbf{w}|\theta)$  is  $N(\mu, \sigma)$  and  $P(\mathbf{w})$  is chosen as  $N(0, \sigma_p)$ .  $\mathbf{w}$  is computed using the reparametrization trick [13] as,  $\mu + \sigma \circ \epsilon$ ,  $\epsilon \sim N(0, 1)$ . Therefore, for this we can analyse the summand in (2) as follows,

- $\log q(\mathbf{w}|\theta)$  - When posterior distribution is  $N(\mu, \sigma)$ , then  $q(\mathbf{w}|\theta)$  can be written as,  $\frac{1}{\sigma\sqrt{2\pi}} \exp(-\frac{1}{2}(\frac{\mathbf{w}-\mu}{\sigma})^2)$ . Since,  $\mathbf{w}$  is  $\mu + \sigma \circ \epsilon$ , hence the term in the exponential part reduces to a constant,  $\exp(\epsilon^2)$ . The only variable in  $q(\mathbf{w}|\theta)$  is therefore,  $\frac{1}{\sigma}$ , hence the variable part of  $\log q(\mathbf{w}|\theta)$  will be,  $-\log(\sigma)$ .
- $\log P(\mathbf{w})$  - When the prior distribution is chosen as  $N(0, \sigma_p)$  then  $P(\mathbf{w})$  can be written as  $\frac{1}{\sigma_p\sqrt{2\pi}} \exp(-\frac{1}{2}(\frac{\mathbf{w}}{\sigma_p})^2)$ . As we have explained above,  $\mathbf{w}$  is  $\mu + \sigma \circ \epsilon$  and the variables are only present in the exponential part, hence,  $\log P(\mathbf{w})$  can be replaced with  $\frac{1}{\sigma_p^2} \mathbf{w}^2$ . Further,  $\mathbf{w}^2$  will be translated to  $\frac{1}{\sigma_p^2}(\mu^2 + \sigma^2 \circ \epsilon^2 + 2\mu \circ \sigma \circ \epsilon)$ . The interesting observation that can be made here is that when  $|\mu \circ \sigma \circ \epsilon| \ll 1$ , then  $\log P(\mathbf{w})$  acts as a L2-regulariser for  $\mu$  and  $\sigma$ . In addition, when  $\mu$  reaches near to an optimal or sub-optimal point,  $\sigma$  tends to 0, so that the approximated

cost in (2) is minimised and the output of the BNN is very close to the expected output [27]. Hence, the assumption  $|\mu \circ \sigma \circ \epsilon| \ll 1$  will hold true in this case.

- $-\log P(D|\mathbf{w})$  - This is simply the negative log likelihood of data given the weights.

We observed from the above analysis that, if  $\mu$  is taken as pre-trained weights of an ANN with point estimate, then the prior distribution over weights is acting as a L2-regulariser for  $\mu$  and if the weights of the previous ANN were already regularised during training then the prior isn't required for learning  $\sigma$ . Therefore, we modified the cost in (2) as follows,

$$F_{mod}(D, \theta) = -\pi_1 \log(\sigma) + \pi_2 E[-\log P(D|\mathbf{w})] + \pi_3 s^2 \quad (3)$$

The cost function in (3) takes  $\mu$  as the weights of an ANN with point estimate and is kept unchanged during training. The only parameter which is optimised is  $\sigma$ . It can be well explained when broken into the following three components,

- $-\pi_1 \log(\sigma)$  - This component ensures that  $\sigma > 0$  during training. The purpose of this is to make sure that  $\sigma \circ \epsilon$  in  $\mu + \sigma \circ \epsilon$  is never zero or the perturbation added to  $\mu$  is never zero.  $\pi_1$  is the importance of this component in  $F_{mod}$ .
- $\pi_2 E[-\log P(D|\mathbf{w})]$  - This is simply the negative log-likelihood of the data given the weights. The importance of this component is controlled by the value of  $\pi_2$ .
- $\pi_3 s^2$  - This is the sum of variances of the softmax scores of each class in different outputs obtained from multiple samples of weights. Specifically if there are  $c$  classes and we took  $n$  Monte Carlo samples of weights, then there will be  $n$  softmax scores and in each of these, the softmax score of  $k^{th}$  class will be different. We take the variance of the scores of each of the  $c$  classes and sum them together to obtain  $s^2$ . In other words, this component reflects the disagreement between the outputs for different samples of weights.  $\pi_3$  is the importance of this component in  $F_{mod}$ .

In short,  $F_{mod}$  in (3) ensures that the perturbations added to the weights of an ANN with point estimate will always be non-zero and will be optimised in such a way that the disagreement between multiple samples of  $\mathbf{w}$  is minimised for the given data without compromising on the test accuracy of the ANN whose weights are being used to learn  $\sigma$ . Optimising  $\sigma$  on  $F_{mod}$  by keeping  $\mu$  fixed will result in *pseudo*-BNN with  $\mu, \sigma$  as its parameters.

Now we propose two measures of disagreement which use multiple outputs from *pseudo*-BNN to effectively segregate OOD and ID inputs.

## 2.2. Measures of Disagreement

Suppose that  $n$  Monte Carlo samples of weights were drawn using *pseudo*-BNN's parameters for classifying the input to  $c$  classes, therefore giving us  $n$  softmax scores for each of the  $c$  classes. Further suppose that, the mean softmax score and it's standard deviation for  $k^{th}$  class is  $\mu_k$  and  $\sigma_k$  respectively. We define the first measure of disagreement as follows,

$$M_1 = -\log\left(\sum_{k=1}^c \frac{\sigma_k}{\mu_k}\right) \quad (4)$$

In (4),  $\frac{\sigma_k}{\mu_k}$  is the index of dispersion of the  $n$  softmax scores for the  $k^{th}$  class. Therefore, in words the measure in (4), attains large values when the sum of index of dispersions for all the classes is low because  $-\log$  is a decreasing function.

In the second measure, we have also included the entropy of the average softmax scores of all the classes as shown below,

$$M_2 = \pi_1 \frac{1}{\sum_{k=1}^c \frac{\sigma_k}{\mu_k}} + \pi_2 \frac{1}{\sum_{k=1}^c -\mu_k \log \mu_k} \quad (5)$$

As it can be observed in (5), the second part of the sum is simply the inversion of the entropy of average softmax scores of all the classes because it can be interpreted as a probability distribution. To ensure that  $M_2$  doesn't becomes inf, a small value close to but greater than zero can be added to  $\sum_{k=1}^c \frac{\sigma_k}{\mu_k}$  and  $\sum_{k=1}^c -\mu_k \log \mu_k$ .

## 3. Related Work

The methods used for OOD input detection can be divided into two broad categories, generative methods which use generative models to flag OOD inputs and classifier methods which use softmax scores for the same task. Our technique belongs to the second category. In this section we have highlighted the previous work from both the categories and wherever possible we have also mentioned how our approach differs from the previous ones.

- A Baseline For Detecting Missclassified And Out-Of-Distribution Examples In Neural Networks [10] - This method is a classifier based method, which aims to utilise the low softmax scores produced by a neural network for misclassified and OOD inputs. It has been shown to work with a variety of datasets and neural networks on diverse sets of tasks including computer vision, natural language processing and automatic speech recognition. This approach differs from

ours in the sense that it only uses the softmax scores produced by a single ANN estimate, where as in ours, we learn a second parameter for injecting random perturbations to the weights of the ANN.

- Enhancing The Reliability Of Out-Of-Distribution Image Detection In Neural Networks [19] - This work is also a classifier based method which builds on top of Hendrycks [10]. It uses temperature scaling and adds small directed perturbations to the inputs, based on the gradient of maximum softmax scores with respect to the input, to effectively separate the softmax scores for ID and OOD inputs. Our approach differs from this work because it doesn't require gradient computation, an expensive operation, to detect OOD inputs.
- A Simple Unified Framework for Detecting Out-of-Distribution Samples and Adversarial Attacks [18] - This work is a generative classifier based method and assumes a multivariate Gaussian distribution over the class conditional distribution. It proposes to use Mahalanobis distance based confidence scores by computing a covariance matrix for each layer and then adding small amount of directed perturbations to the input and then computing their proposed confidence scores, which at the end are fed to a logistic regressor. The logistic regressor is trained with the help of validation samples. Our approach doesn't assume anything about the distributions of the outputs from any layer and relies completely on the final predictions made by the *pseudo*-BNN.
- Likelihood Ratios for Out-of-Distribution Detection [23] - This method assumes that an input is composed of two components, a *background* component and a *semantic* component and trains two models,  $p_\theta$  on ID data and  $p_{\theta_o}$  is a background model which captures background statistics. Then a likelihood ratio statistic defined as  $\log \frac{p_\theta(\mathbf{x})}{p_{\theta_o}(\mathbf{x})}$  to detect OOD inputs by comparing it with a threshold. It has been shown to work with image and genomic datasets.
- For OOD detection, ensemble based techniques which use predictions from more than one neural networks to classify an input as OOD. However, scaling this technique to large networks is difficult due to its high memory requirements. In addition, entropy of the softmax scores have also been used previously to detect OOD inputs. There have also been attempts to use an ensemble of generative models and evaluating  $E[\log p_\theta(\mathbf{x})] - \text{Var}[\log p_\theta(\mathbf{x})]$  [6]. Our approach though measures disagreement between multiple outputs but they are obtained from multiple samples of weights from a single neural network.

## 4. Experiments and Results

We first trained an ANN on a dataset to obtain point estimate and then trained a *pseudo*-BNN by reusing the weights of the previously trained ANN as  $\mu$  and optimising the cost function in (3) over  $\sigma$  for the same dataset. We used the following combination of architectures and ID datasets in our experiments,

- $C_1$  - A simple CNN architecture with first two layers of Convolution layers with a common kernel size of (5, 5) and number of channels as 32 and 64 and a stride of 1 with SAME padding. We used max pooling of window size (2, 2) and with a stride of 2, after each convolution layer. The last two layers were fully connected with 1024 and 10 output units respectively. All but last layer used ReLU activation. The dataset used for training was MNIST database of handwritten digits. We trained *pseudo*-BNN for 1708 iterations with a batch size of 256.
- $C_2$  - VGG-10 was trained on CIFAR10 dataset. For training *pseudo*-BNN, we used 1712 iterations with a batch size of 64.
- $C_3$  - ResNet-20 was trained on CIFAR10 dataset. Here, for *pseudo*-BNN, we ran 802 iterations with a batch size of 128.
- $C_4$  - A simple CNN architecture was trained on SVHN dataset. It had a sequence of Convolution-Batch Normalisation-Convolution-Max Pool-Dropout blocks. There were three such blocks with 32, 64 and 128 channels in the Convolution layers. The kernel size of all the Convolution layers was (3, 3) with a stride of 1 and SAME padding. The window size for Max Pool was (2, 2) with a stride of 1. The Dropout rate was 0.3. The last two layers were fully connected with 128 and 10 output units. For *pseudo*-BNN, we ran 315 iterations with a batch size of 128.
- $C_5$  - DenseNet-100 with a growth rate of 12 was trained on CIFAR100 dataset. For *pseudo*-BNN model of this architecture, we used 120 iterations with a batch size of 64.

Instead of learning  $\sigma$ , we also tried another approach where we added small random perturbations to the weights of a frequentist ANN but we observed that this approach results in degradation of test accuracy if the strength of perturbations is high and if it is low then test accuracy is preserved but the performance of OOD input detection degrades. For example, when we added perturbations sampled from  $N(0, 1)$  to the weights ANN model of  $C_1$  architecture, the test accuracy on MNIST dataset [17] reduced from  $\approx 98\%$  to  $\approx 10\%$  and when we sampled the perturbations

Architecture	ID/OOD	Method	FPR at 95 % TPR $\downarrow$	AUPR $\uparrow$	AUROC $\uparrow$	Detection Error $\downarrow$
$C_1$	MNIST/ Fashion-MNIST	Ours ( $M_1$ )	<b>1.72</b>	<b>99.44</b>	99.32	<b>3.36</b>
		Hendrycks [10]	27.48	97.00	96.06	16.24
		ODIN	27.088	96.92	96.00	16.05
		MHB	30.31	96.49	95.31	17.65
		LLR( $\mu$ ) <sup>*</sup>	NA	95.10	97.30	NA
		LLR( $\mu, \lambda$ ) <sup>*</sup>	NA	99.30	<b>99.40</b>	NA
$C_2$	CIFAR10/ CMATERDB	WAIC(5 models) <sup>*</sup>	NA	40.10	22.10	NA
		Ours ( $M_2$ )	<b>54.80</b>	<b>95.98</b>	91.53	<b>29.87</b>
		Hendrycks [10]	61.48	92.58	91.82	33.23
		ODIN	56.80	93.11	<b>92.48</b>	30.89
$C_2$	CIFAR10/ CIFAR100	MHB	100.0	62.008	47.32	52.52
		Ours ( $M_2$ )	<b>67.41</b>	<b>88.92</b>	87.45	<b>36.21</b>
		Hendrycks [10]	71.35	82.56	88.65	38.17
		ODIN	71.39	82.88	<b>88.70</b>	38.19
$C_3$	CIFAR10/ CMATERDB	MHB	99.86	40.89	34.36	52.447
		Ours ( $M_2$ )	<b>48.18</b>	<b>92.41</b>	<b>92.62</b>	<b>26.58</b>
		Hendrycks [10]	58.88	90.68	90.13	31.94
		ODIN	59.03	90.10	89.71	32.02
$C_3$	CIFAR10/ CIFAR100	MHB	75.63	90.60	87.64	40.32
		Ours ( $M_2$ )	<b>64.37</b>	<b>98.82</b>	<b>91.36</b>	<b>34.69</b>
		Hendrycks [10]	70.74	85.89	85.96	37.87
		ODIN	71.6	85.63	85.87	38.30
$C_4$	SVHN/ CIFAR10	MHB	99.71	50.74	44.36	52.36
		Ours ( $M_2$ )	<b>37.00</b>	<b>94.85</b>	93.01	<b>21.00</b>
		Hendrycks [10]	43.80	93.12	<b>94.04</b>	24.44
		ODIN	43.18	93.02	94.00	24.09
$C_4$	SVHN/ CMATERDB	MHB	88.50	92.70	89.06	46.75
		Ours ( $M_2$ )	51.00	<b>87.73</b>	92.06	28.00
		Hendrycks [10]	<b>49.00</b>	84.93	<b>92.34</b>	<b>27.00</b>
		ODIN	52.59	84.49	92.04	28.80
$C_4$	SVHN/ GAUSSIAN	MHB	87.083	87.68	84.84	40.02
		Ours ( $M_2$ )	<b>1.61</b>	<b>98.51</b>	<b>98.85</b>	<b>3.31</b>
		Hendrycks [10]	19.95	98.00	96.88	12.48
		ODIN	19.97	97.92	96.85	12.48
$C_5$	CIFAR100/ CIFAR10	MHB	95.08	91.41	86.45	50.04
		Ours ( $M_2$ )	89.62	<b>73.00</b>	70.20	47.33
		Hendrycks [10]	<b>87.77</b>	70.99	<b>70.88</b>	<b>46.38</b>
		ODIN	87.98	70.65	70.71	46.5
$C_5$	CIFAR100/ CMATERDB	MHB	98.45	47.32	43.48	51.72
		Ours ( $M_2$ )	81.7	82.73	77.68	43.36
		Hendrycks [10]	82.80	80.81	77.07	43.89
		ODIN	82.60	81.41	77.52	43.81
		MHB	<b>0.43</b>	<b>99.65</b>	<b>99.53</b>	<b>2.71</b>

Table 1. The performance of various methods on OOD input detection using various neural network architectures and datasets.  $C_1$  and  $C_4$  are simple convolution architectures.  $C_2$  is VGG-10,  $C_3$  is ResNet-20 and  $C_5$  is DenseNet-100 with growth rate of 12. Ours denotes our proposed technique, ODIN refers to Lieang *et al.* [19], MHB refers to Lee *et al.* [18], LLR refers to Ren *et al.* [23], and WAIC refers to Choi *et al.* [6]. The best results for each ID/OOD dataset and architecture combination is highlighted in bold. \* denotes the directly reported results. We tried both  $M_1$  and  $M_2$  for our technique and show the best results here.

from  $N(0, 0.01)$ , the FPR at 95% TPR for Fashion-MNIST was  $\approx 55\%$ . By learning  $\sigma$ , we were able to achieve, 1.72%

FPR at 95% TPR as shown in Table 1. In fact, handcrafting the strength of perturbations is nearly impossible because

Architecture	Dataset	Test Accuracy of ANN (in %)	Test Accuracy of <i>pseudo</i> -BNN (in %)
$C_1$	MNIST	98.53	98.49
$C_2$	CIFAR10	93.54	93.66
$C_3$	CIFAR10	91.68	91.44
$C_4$	SVHN	95.93	94.43
$C_5$	CIFAR100	68.099	68.08

Table 2. The test accuracy of an ANN with point estimate and the associated *pseudo*-BNN for various architectures.  $C_1$  and  $C_4$  are simple convolution architectures.  $C_2$  is VGG-10,  $C_3$  is ResNet-20 and  $C_5$  is DenseNet-100 with growth rate of 12.

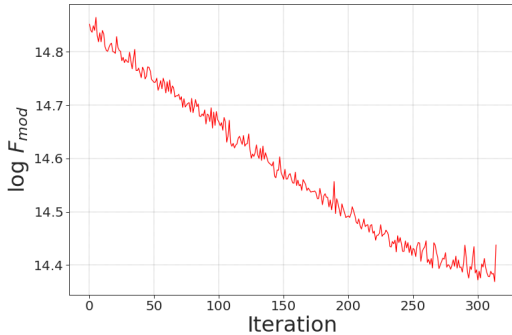


Figure 1.  $\log F_{mod}(3)$  vs Iteration for  $C_4$  architecture with SVHN as training data.

in complex neural network architectures it is very difficult to predict the effect of perturbing weights on the outputs if done manually. Our proposed cost function automates this process and  $\sigma$  is learnt in such a way that both the requirements of OOD input detection and test accuracy are satisfied.

To ensure that  $\sigma > 0$  during optimisation of (3), we parametrise it using  $\rho$  as,  $\sigma = \log 1 + \exp \rho$ . The optimizer used for all but last architecture was *RMSprop* [26] with a learning rate of 0.01. We used SGD with a learning rate of 0.01 for the DenseNet-100 architecture. The values of  $\pi_1$  and  $\pi_3$  in (3) were always 1 and that of  $\pi_2$  was adjusted such that it attains values approximately  $\frac{1}{10}^{th}$  of  $-\log \sigma$ . We stopped the training when either the negative log likelihood, cross entropy for image classification tasks, started to increase or there wasn't any further decrease in  $\pi_3 s^2$  (third component in (3)). The intuition behind this is that optimising  $\sigma$  in further iterations won't be beneficial because, increasing  $\sigma$  will either fluctuate the outputs for ID data too much and decreasing  $\sigma$  will increase  $-\log \sigma$ . In Fig. 1 we show how the total cost decreases while training *pseudo*-BNN model of  $C_4$  architecture with SVHN as training data. It can be seen that initially the cost decreases but towards the end the fluctuations in the cost increases and hence we stopped the training for further iterations.

In Table 2, we show the differences in test accuracy of

ANNs with point estimate and *pseudo*-BNN for the above architectures. Only one sample of weights was drawn for computing these test accuracy. It can be observed that the change in test accuracy is negligible as compared to their counterparts. In Table 1, we show the results from our technique for OOD input detection and compare it with previous work on metrics such as False Positive Rate at 95 % True Positive Rate (FPR at 95 % TPR), Area Under the Precision Recall Curve (AUPR), Area Under the Receiver Operating Characteristic Curve (AUROC) and Detection Error. These metrics have been used for evaluation in [10, 19, 18, 23]. For ODIN [19], we picked  $T$  for temperature scaling from,  $\{10, 100, 1000\}$  and  $\epsilon$  from  $\{0.0001, 0.00625, 0.025, 0.05, 0.1\}$ . In Mahalanobis Distance [18], we used the outputs from the second last and last layer. It is to be noted that, no method, including ours, was adapted to OOD data beforehand for better performance, because at the time of deployment, OOD examples can come from any distribution and fine tuning a method for one distribution may not guarantee performance for other distributions. It can be seen that, our method beats the previous work on most of the datasets and neural network architectures and achieves comparable results in other cases. Mahalanobis distance [18] is observed to perform well when CIFAR100 is ID dataset and CMATERDB is OOD dataset and the architecture used is DenseNet-100 with a growth rate of 12. The reason behind poor performance of other techniques, including ours might be due to poor training of the model, which is a solvable issue.

In Fig. 2, it can be seen that using  $M_1$  (4) on the outputs of *pseudo*-BNN model of  $C_1$  architecture, the MNIST and Fashion-MNIST are almost clearly segregated from each and hence verifying the results. In addition, for the the same setup, Fig. 3, the FPR at 95% TPR is the least for ours among all the methods.

## 5. Principled Analysis

In *pseudo*-BNN, at the time of inference, we compute,  $w$  using  $\mu + \sigma \circ \epsilon$ ,  $\epsilon \sim N(0, 1)$ . We can interpret this as  $\sigma \circ \epsilon$  amount of perturbation added to  $\mu$ . On the basis of this interpretation, we learn  $\sigma$  by optimising the cost function in (3) by keeping  $\mu$  as the weights of a pre-trained ANN.

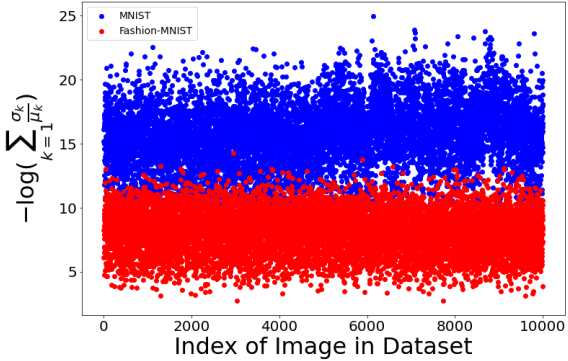


Figure 2. Segregation of MNIST (ID) and Fashion-MNIST (OOD) images using *pseudo*-BNN model of architecture  $C_1$  and measure of disagreement  $M_1$  (4).

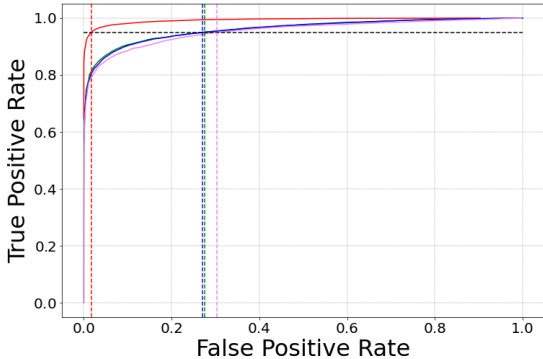


Figure 3. True Positive Rate v/s False Positive Rate curves of different methods for MNIST as ID and Fashion-MNIST as OOD data using  $C_1$  architecture. The red curve is our method, green curve is Baseline [10], blue curve is ODIN [19] and the violet curve is Mahalanobis Distance [18]. It can be seen that the False Positive Rate at 95 % True Positive Rate is least for our method.

$\mu$  is kept fixed during the whole training process. If the loss function, categorical cross entropy for classifier neural networks, is denoted as  $L(\mathbf{w})$ , the gradient with respect to the weights and their perturbations in the  $k^{th}$  layer as  $g(\mathbf{w}_k)$  and  $\Delta\mathbf{w}_k$  and if there are  $l$  layers in the neural network, then by fundamental theorem of calculus the following holds [2]

$$L(\mathbf{w} + \Delta\mathbf{w}) - L(\mathbf{w}) = \sum_{k=1}^l \int_0^1 g(\mathbf{w}_k + t\Delta\mathbf{w}_k)^T \Delta\mathbf{w}_k dt \quad (6)$$

Using (6) we can derive the lower and upper bounds for  $L(\mathbf{w} + \Delta\mathbf{w})$  as shown in (7), (8) and empirically in Fig. 4.

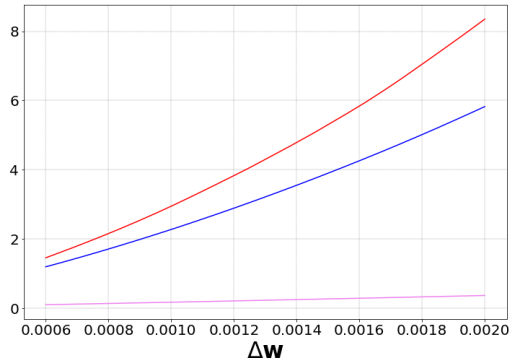
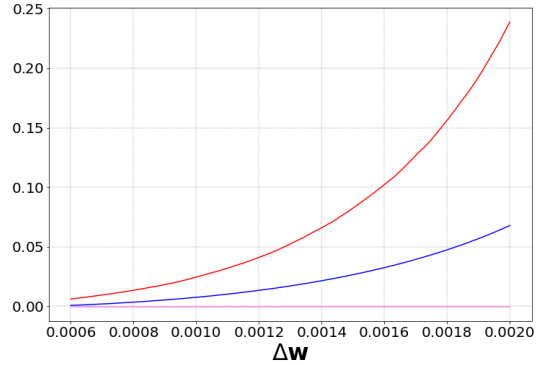


Figure 4. The change in the loss for ID data (top) and OOD data (bottom) due to addition of  $\Delta\mathbf{w}$  to  $\mathbf{w}$ . The red line is  $\max_t \sum_{k=1}^l g(\mathbf{w}_k + t\Delta\mathbf{w}_k)^T \Delta\mathbf{w}_k$ , violet line is  $\min_t \sum_{k=1}^l g(\mathbf{w}_k + t\Delta\mathbf{w}_k)^T \Delta\mathbf{w}_k$  and blue line is  $L(\mathbf{w} + \Delta\mathbf{w}) - L(\mathbf{w})$ .

$$L(\mathbf{w} + \Delta\mathbf{w}) - L(\mathbf{w}) \leq \max_t \sum_{k=1}^l g(\mathbf{w}_k + t\Delta\mathbf{w}_k)^T \Delta\mathbf{w}_k \quad (7)$$

$$\min_t \sum_{k=1}^l g(\mathbf{w}_k + t\Delta\mathbf{w}_k)^T \Delta\mathbf{w}_k \leq L(\mathbf{w} + \Delta\mathbf{w}) - L(\mathbf{w}) \quad (8)$$

The significance of (7) and (8) is that the change in the loss due to perturbations added to the weights of a neural network is bounded from above and below by the maximum and the minimum values of sum of the dot products of the strength of the gradients and the perturbations in weights of all layers. If the perturbations are the same, then for OOD input the gradients will be higher because the neural network was never optimised for it but for ID input, the gradient will be low because, it is the ID dataset on which the neural network was trained. This intuitively explains the

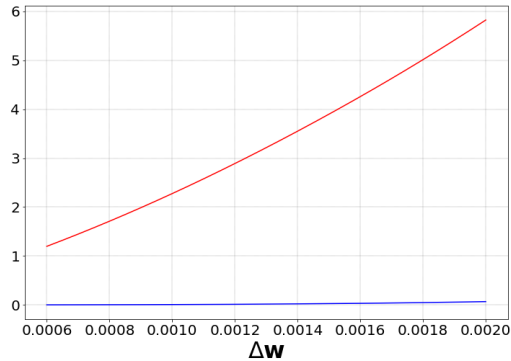


Figure 5. Comparison of changes in the loss for OOD and ID data due to addition of  $\Delta w$  to  $w$ . The red line is change in loss for OOD data and blue for ID data. It can be noted that for same  $\Delta w$  the change in loss for OOD data is significantly greater as compared to ID data.

working of our technique that is for OOD input, the output of *pseudo*-BNN fluctuates more than the outputs for ID input. Fig. 5 shows that the change in loss for OOD inputs is much greater than that for ID inputs.

## 6. Conclusion

In this paper, we proposed a new cost function for training a modified form of conventional BNNs. We also proposed two measures of disagreement for effectively segregating, ID and OOD inputs. The advantages offered by our work can be listed as follows,

- As shown in our experiments, converting an ANN with point estimate to *pseudo*-BNN requires very little training effort. This avoids the hard work of re-training all of the state of the art networks for OOD detection from scratch.
- We used only 2 to 5 samples of weights from *pseudo*-BNN to detect OOD inputs which results in a very little overhead with respect to the inference time but increases the safety of neural networks significantly. As compared to previous work which used gradient computation, a memory expensive operation as compared to matrix multiplication, our approach is more efficient and incurs a very little memory cost by introducing only a second parameter.
- For training a *pseudo*-BNN, selecting a good prior, which is a problem in conventional BNNs, isn't a requirement anymore. The proposed measures effectively utilise the differences in the outputs for multiple samples of weights for the same input to segregate ID and OOD inputs.

## References

- [1] Dario Amodei, Chris Olah, Jacob Steinhardt, Paul Christiano, John Schulman, and Dan Mané. Concrete problems in ai safety. *arXiv preprint arXiv:1606.06565*, 2016. 1
- [2] Jeremy Bernstein, Jiawei Zhao, Markus Meister, Ming-Yu Liu, Anima Anandkumar, and Yisong Yue. Learning compositional functions via multiplicative weight updates. *Advances in Neural Information Processing Systems*, 33, 2020. 2, 7
- [3] Charles Blundell, Julien Cornebise, Koray Kavukcuoglu, and Daan Wierstra. Weight uncertainty in neural networks. *arXiv preprint arXiv:1505.05424*, 2015. 2
- [4] Kumar Chellapilla, Sidd Puri, and Patrice Simard. High performance convolutional neural networks for document processing. 2006. 1
- [5] Kyunghyun Cho, Bart Van Merriënboer, Caglar Gulcehre, Dzmitry Bahdanau, Fethi Bougares, Holger Schwenk, and Yoshua Bengio. Learning phrase representations using rnn encoder-decoder for statistical machine translation. *arXiv preprint arXiv:1406.1078*, 2014. 1
- [6] Hyunsun Choi, Eric Jang, and Alexander A Alemi. Waic, but why? generative ensembles for robust anomaly detection. *arXiv preprint arXiv:1810.01392*, 2018. 4, 5
- [7] Nibaran Das, Jagan Mohan Reddy, Ram Sarkar, Subhadip Basu, Mahantapas Kundu, Mita Nasipuri, and Dipak Kumar Basu. A statistical-topological feature combination for recognition of handwritten numerals. *Appl. Soft Comput.*, 12(8):2486–2495, Aug. 2012. 2
- [8] Jean Daunizeau. The variational laplace approach to approximate bayesian inference. *arXiv preprint arXiv:1703.02089*, 2017. 2
- [9] Kaiming He, Xiangyu Zhang, Shaoqing Ren, and Jian Sun. Deep residual learning for image recognition. In *Proceedings of the IEEE conference on computer vision and pattern recognition*, pages 770–778, 2016. 1
- [10] Dan Hendrycks and Kevin Gimpel. A baseline for detecting misclassified and out-of-distribution examples in neural networks. *arXiv preprint arXiv:1610.02136*, 2016. 1, 2, 3, 4, 5, 6, 7
- [11] Gao Huang, Zhuang Liu, Laurens Van Der Maaten, and Kilian Q Weinberger. Densely connected convolutional networks. In *Proceedings of the IEEE conference on computer vision and pattern recognition*, pages 4700–4708, 2017. 2
- [12] Tommi S Jaakkola and Michael I Jordan. Bayesian parameter estimation via variational methods. *Statistics and Computing*, 10(1):25–37, 2000. 2
- [13] Diederik P Kingma and Max Welling. Auto-encoding variational bayes, 2014. 1, 2
- [14] Alex Krizhevsky, Vinod Nair, and Geoffrey Hinton. Cifar-10 (canadian institute for advanced research). 2
- [15] Alex Krizhevsky, Vinod Nair, and Geoffrey Hinton. Cifar-100 (canadian institute for advanced research). 2
- [16] Alex Krizhevsky, Ilya Sutskever, and Geoffrey E Hinton. Imagenet classification with deep convolutional neural networks. In F. Pereira, C. J. C. Burges, L. Bottou, and K. Q.

Weinberger, editors, *Advances in Neural Information Processing Systems*, volume 25, pages 1097–1105. Curran Associates, Inc., 2012. 1

[17] Yann LeCun, Corinna Cortes, and CJ Burges. Mnist handwritten digit database. *ATT Labs [Online]. Available: <http://yann.lecun.com/exdb/mnist>*, 2, 2010. 2, 4

[18] Kimin Lee, Kibok Lee, Honglak Lee, and Jinwoo Shin. A simple unified framework for detecting out-of-distribution samples and adversarial attacks. In *Advances in Neural Information Processing Systems*, pages 7167–7177, 2018. 4, 5, 6, 7

[19] Shiyu Liang, Yixuan Li, and Rayadurgam Srikant. Enhancing the reliability of out-of-distribution image detection in neural networks. *arXiv preprint arXiv:1706.02690*, 2017. 4, 5, 6, 7

[20] Radford M Neal and Geoffrey E Hinton. A view of the em algorithm that justifies incremental, sparse, and other variants. In *Learning in graphical models*, pages 355–368. Springer, 1998. 2

[21] Yuval Netzer, Tao Wang, Adam Coates, Alessandro Bissacco, Bo Wu, and Andrew Y Ng. Reading digits in natural images with unsupervised feature learning. *Advances in Neural Information Processing Systems (NIPS)*, 2011. 2

[22] Anh Nguyen, Jason Yosinski, and Jeff Clune. Deep neural networks are easily fooled: High confidence predictions for unrecognizable images. In *Proceedings of the IEEE conference on computer vision and pattern recognition*, pages 427–436, 2015. 1

[23] Jie Ren, Peter J Liu, Emily Fertig, Jasper Snoek, Ryan Poplin, Mark Depristo, Joshua Dillon, and Balaji Lakshminarayanan. Likelihood ratios for out-of-distribution detection. In *Advances in Neural Information Processing Systems*, pages 14707–14718, 2019. 4, 5, 6

[24] Lawrence K Saul, Tommi Jaakkola, and Michael I Jordan. Mean field theory for sigmoid belief networks. *Journal of artificial intelligence research*, 4:61–76, 1996. 2

[25] Karen Simonyan and Andrew Zisserman. Very deep convolutional networks for large-scale image recognition. *arXiv preprint arXiv:1409.1556*, 2014. 1

[26] T. Tieleman and G. Hinton. Lecture 6.5—RmsProp: Divide the gradient by a running average of its recent magnitude. COURSERA: Neural Networks for Machine Learning, 2012. 6

[27] R. J. Williams. Simple statistical gradient-following algorithms for connectionist reinforcement learning. *Machine Learning*, 8:229–256, 1992. 3

[28] Han Xiao, Kashif Rasul, and Roland Vollgraf. Fashion-mnist: a novel image dataset for benchmarking machine learning algorithms. *CoRR*, abs/1708.07747, 2017. 2

[29] Jonathan S Yedidia, William Freeman, and Yair Weiss. Generalized belief propagation. *Advances in neural information processing systems*, 13:689–695, 2000. 2

[30] Chiyuan Zhang, Samy Bengio, Moritz Hardt, Benjamin Recht, and Oriol Vinyals. Understanding deep learning requires rethinking generalization. *arXiv preprint arXiv:1611.03530*, 2016. 1